PHILOSOPHICAL TRANSACTIONS B

royalsocietypublishing.org/journal/rstb

Research

Cite this article: Schaal SM, Haller BC, Lotterhos KE. 2022 Inversion invasions: when the genetic basis of local adaptation is concentrated within inversions in the face of gene flow. *Phil. Trans. R. Soc. B* **377**: 20210200.
https://doi.org/10.1098/rstb.2021.0200

Received: 14 December 2021
Accepted: 9 May 2022

One contribution of 15 to a theme issue 'Genomic architecture of supergenes: causes and evolutionary consequences'.

Subject Areas:
evolution

Keywords:
structural rearrangements, low recombination, local adaptation, polygenic adaptation

Author for correspondence:
Sara M. Schaal
e-mail: schaal.s@northeastern.edu

Electronic supplementary material is available online at https://doi.org/10.6084/m9.figshare.c.5995957.

THE ROYAL SOCIETY PUBLISHING

Inversion invasions: when the genetic basis of local adaptation is concentrated within inversions in the face of gene flow

Sara M. Schaal[1], Benjamin C. Haller[2] and Katie E. Lotterhos[1]

[1]Department of Marine and Environmental Sciences, Northeastern University, Nahant, MA, USA
[2]Department of Computational Biology, Cornell University, Ithaca, NY, USA

SMS, 0000-0001-5986-0193; KEL, 0000-0001-7529-2771

Across many species where inversions have been implicated in local adaptation, genomes often evolve to contain multiple, large inversions that arise early in divergence. Why this occurs has yet to be resolved. To address this gap, we built forward-time simulations in which inversions have flexible characteristics and can invade a metapopulation undergoing spatially divergent selection for a highly polygenic trait. In our simulations, inversions typically arose early in divergence, captured standing genetic variation upon mutation, and then accumulated many small-effect loci over time. Under special conditions, inversions could also arise late in adaptation and capture locally adapted alleles. Polygenic inversions behaved similarly to a single supergene of large effect and were detectable by genome scans. Our results show that characteristics of adaptive inversions found in empirical studies (e.g. multiple large, old inversions that are F_{ST} outliers, sometimes overlapping with other inversions) are consistent with a highly polygenic architecture, and inversions do not need to contain any large-effect genes to play an important role in local adaptation. By combining a population and quantitative genetic framework, our results give a deeper understanding of the specific conditions needed for inversions to be involved in adaptation when the genetic architecture is polygenic.

This article is part of the theme issue 'Genomic architecture of supergenes: causes and evolutionary consequences'.

1. Introduction

A major goal of evolutionary biology is to understand how populations adapt to spatial variation in environmental conditions. Although local adaptation (LA) at large spatial scales is commonly observed, we still lack an understanding of how LA evolves at the genetic level when gene flow is high [1]. Through the study of ecotypes and sympatric population pairs, we now have a growing body of evidence that suggests inversion polymorphisms may play an important role in harbouring the genetic basis of LA [2–5]. However, we are still lacking detailed theoretical support for the genetic architectures that evolve within inversions under different levels of gene flow.

When a genomic region becomes inverted, it results in a standard and an inverted arrangement in the population. If an individual is heterozygous for the inversion, gene flow is effectively reduced due to the loss of the unbalanced gametes [6–8]. Thus, locally beneficial combinations of alleles can be shielded from the homogenizing effects of gene flow when occurring within an inverted region [2]. Empirical evidence supports this hypothesis, with inversions being outliers in genome scans for ecotype comparisons across the tree of life (see review: [3,9–16]). Additionally, these studies have observed that multiple, long inversions that established early in divergence are involved in LA. To date, modelling efforts have not been able to explain why multiple adaptive inversions evolve. In addition, recombination variation can challenge genome

Table 1. List of terms used in the manuscript and how we defined them.

adaptive inversion window	inversion window that did meet the three criteria for concentration of divergence within the inversion (from *selection simulation*, see electronic supplementary material, S2 for criteria)
collinear	part of the genome that is outside of inverted windows (i.e. the non-inverted genome)
genomic clustering	a group of QTN loci that are in close physical linkage with one another and exhibit elevated divergence relative to the rest of the genome
inversion haplotype alleles (for individual *i*)	alleles at QTNs found in an inverted arrangement for individual *i*
inversion window	span of the genetic map in which an inversion is present in the metapopulation
inversion window QTNs	all QTNs found within an inversion window that is present in the metapopulation
mean inversion effect size	mean additive effect of the inverted arrangement on the phenotype averaged across all copies of the inverted arrangement
no-inversion control simulation	simulations without inversions where spatially divergent selection is acting on the quantitative trait (control for adaptation dynamics due solely to inversions)
no-selection control simulation	neutral simulations where individuals all had equal fitness but inversions were occuring (control for inversion dynamics due solely to migration, mutation and drift)
no-selection inversion window	*inversion window* in the no-selection control simulations (used as a control to compare to inversion selection simulations)
nonadaptive inversion window	inversion window that did not meet the three criteria for concentration of divergence within the inversion (from *selection simulation*, see electronic supplementary material, S2 for criteria)
QTN	quantitative trait nucleotide (single base): the derived allele has a causal effect on the phenotype, while the ancestral allele is neutral
selection simulation	simulations with inversions where spatially divergent selection is acting on the quantitative trait

scans, and questions remain as to whether some of these examples could be statistical artefacts [17,18].

Inversion polymorphisms have been observed when LA is occurring in the face of high levels of gene flow, but current models have yet to evaluate the mechanisms underlying this process. To date, models have focused on conditions in which inversions capture all like-effect, locally adapted alleles, which typically requires some period of allopatry (i.e. zero gene flow) for inversions to aid in LA [19–22]. This theory showed that inversions are likely to establish when the loci they capture are weakly linked and under weak selection [19,23]. Closely linked alleles experiencing low recombination can behave as a large-effect locus [24] and in this case the inversion does not offer an advantage [23] because the alleles are not prone to swamping by migration (hereafter: swamping-resistant alleles; swamping occurs when a locus is unable to overcome the homogenizing effect of gene flow, resulting in the loss of genetic variance at a locus under selection [25,26]). These models, however, assumed a period of allopatry.

No modelling study has explored the possibility for inversions to facilitate adaptation under high gene flow, as we see empirically in species like Atlantic cod (*Gadus morhua*) and monkey flower (*Mimulus guttatus*; [10,11,27]). Recent simulations have illustrated the importance of the accumulation of small-effect alleles in LA under high gene flow [26,28]. A highly polygenic, genotypically redundant (as in [29]) architecture can allow for LA to occur even when the alleles are individually prone to swamping by migration (hereafter: swamping-prone alleles; [27]). Therefore, the question remains as to whether genomes with multiple, large and old inversions involved in LA under high gene flow could be consistent with a highly polygenic architecture, and whether inversions could establish as a means of accumulation (as opposed to capture, as previous theory/simulations have assumed) of small-effect alleles [30].

Empirical studies have identified that putatively adaptive inversion polymorphisms tend to be long (range in size from approx. 100 kb–100 mb; reviewed in [3]). Previous simulations have mainly evaluated inversions of fixed length ([20–22], but see continent-island model [31]), and this limits the inferences that can be made due to the unexplored interplay between length and the possibility to capture both adaptive and maladaptive loci. If a phenotype is highly polygenic, longer inversions that capture quantitative trait nucleotides (QTNs; table 1) could be more likely to capture alleles with opposing effects on a phenotype and therefore, smaller inversions that capture the right combination of alleles might be more prevalent. On the other hand, theory predicts that adaptive alleles arise near each other because of higher establishment probabilities [32], and therefore longer inversions might have a higher probability of establishment if they arise neutrally and accumulate QTNs through mutation [32].

Putatively adaptive inversions can be millions of years old, but their origins have been debated. In species where ecotype differentiation predated the inversion, researchers concluded that the inversion captured a beneficial combination of locally adapted alleles at the time the inversion mutated ('capture'; [11,33]). Conversely, other empirical studies found that accumulation of mutations inside an inversion over time caused it to establish and persist in the population ('gain'; [12]). Since previous simulation studies focused on the capture

dynamics of inversions introduced at a specific period of time [19,20,22,23,34], they lacked the flexibility to explain these empirical observations.

Another empirical observation that is not well explained by current models is the involvement of overlapping inversions in LA. While overlapping inversions were observed in insects as early as the 1950s using karyotyping [35–37], it was not until recently that overlapping inversions were discovered to play a role in LA in diverse taxa (e.g. [13,38,39]). In 1953, Wallace [40] argued there should be selection against overlapping inversions, due to the formation of aneuploid gametes and the disruption of blocks of genes. Wallace predicted that overlapping inversions can only be maintained by selection, but the field currently lacks models to test this prediction.

To better understand the mechanisms through which inversion polymorphisms facilitate LA under polygenic architectures and the potential for statistical artefacts, we built a novel set of forward-time quantitative genetic simulations that allow for both QTN and inversion mutations to arise and either persist or be lost due to swamping or drift. Our simulations improve upon previous models (see electronic supplementary material, S1 for comparison of our model to some relevant models) because inversions of a range of sizes can mutate each generation, inversion mutations can arise anywhere in the genome, and the genetic architecture of the trait can evolve. Additionally, our combined population and quantitative genetic framework allows us to partition the additive genetic variance (V_A) for a trait between inverted versus collinear genomic regions (non-inverted; table 1).

We compare simulations with and without inversion mutations across a range of parameters, to ask five main questions: (Q1) Under what conditions do inversions increase the degree of LA under gene flow? (Q2) Under what conditions is divergence concentrated within inversions? (Q3) What are the characteristics of adaptive inversions? (Q4) For an adaptive inversion to segregate and persist under LA with gene flow, must it capture QTNs initially? (Q5) Do outlier tests reliably detect adaptive inversions? To meet a high level of rigour, we included multiple types of controls in our study (neutral segments within the same genome, control simulations with inversions but without selection, control simulations without inversions but with selection). These controls allowed us to identify adaptive inversions that contributed disproportionately to divergence and compare them to (i) the collinear genome, (ii) nonadaptive inversions and (iii) the neutral genome. We elucidated the conditions under which long inversions evolved early in divergence, captured multiple small-effect loci at the time of mutation, and gained small-effect loci over time, which led them to behave similarly to a single large-effect supergene complex of loci.

2. Methods

(a) Simulation model

We simulated a two-patch, Wright–Fisher, forward-time simulation using SLiM (v. 3.6; [41]). Rather than run every simulation to equilibrium, our goal was to compare inversion dynamics across a wide parameter space after a large number of generations. We simulated 21 linkage groups (LGs), each 10 centimorgans (cM) long, with a resolution of 0.0001 cM between proximate bases in SLiM. In 20 of the LGs QTN mutations could arise, and the 21st was neutral. Thus, our simulations represented the case where unlinked regions of the genome affected by selection were tracked within a much larger (untracked) genome. The recombination rate (crossover rate) was scaled to mimic the case where SNPs were collected across each LG (similar to a SNP chip), but still low enough to allow signatures of selection to arise in neutral loci linked to selected loci (in the simulations 100 000 bases was 10 cM; in humans 100 000 bp would correspond to 0.1 cM). Our demes consisted of $N = 1000$ diploid individuals in each deme, and the population-scaled mutation rate $N_e\mu$ for QTNs whose effect size was drawn from a normal distribution with a mean of 0 and standard deviation of σ_m depended on the parameter level: for 'polygenic' $N_e\mu = 0.00002$ and $\sigma_m = 0.2$ (lower mutation rate and larger effect size of mutations); for 'highly polygenic' $N_e\mu = 0.0002$ and $\sigma_m = 0.002$ (higher mutation rate and smaller effect size of mutations); which are on the scale that lead to evolution of polygenic architectures [26,42]. We simulated six levels of migration ranging from low migration to panmixia ($m = \{0.001, 0.01, 0.1, 0.25, 0.4, 0.5\}$) and included simulations with and without environmental variance added to individual phenotypes ($\sigma_{env} = \{0, 0.1\}$). The phenotype of a given individual i in deme p was calculated as the sum of the QTN effect sizes (α) across all QTN loci (n_j) in their genome with the addition of environmental variance:

$$z_{ip} = \sum_{j=1}^{n_j}\sum_{k=1}^{2}\alpha_{kjip} + \epsilon_{ip} \tag{2.1}$$

where α_{kjip} was the effect size of allele k at locus j in individual i in deme p, and $\epsilon_{ip} = N(0, \sigma_{\text{env}})$ was environmental noise added to the trait value for that individual. Phenotypes were under stabilizing selection, with an individual's fitness w_i in a given deme p governed by a Gaussian fitness function:

$$w_{ip} = 1 - \exp\left(\frac{(z_{ip} - \Theta_p)^2}{\omega_p^2}\right) \tag{2.2}$$

where Θ_p represented the deme-specific phenotypic optimum and ω_p^2 represented the strength of stabilizing selection on the trait. We simulated three strengths of selection corresponding to the width of the stabilizing fitness function (i.e. $\omega_p = \{0.75$ (strong), 1.5 (moderate), 3.0 (weak)$\}$). Demes were made up of non-overlapping generations and were connected via a migration rate m. After migration, individuals were chosen to reproduce in each deme with a probability proportional to their fitness, and offspring were produced from parental gametes after mutation and recombination (see electronic supplementary material, S2, section I.A. for further details on order of events). At the start of each simulation, we simulated a 10 000 generation neutral burn-in period that allowed standing genetic variation to arise. After that period, the demes were given phenotypic optima (Θ_p) of +1 and −1. A summary of all parameters and variables used in the simulations can be found in electronic supplementary material, S2, table S1. Each parameter combination was run for five replicate simulations over 60 000 (30 N) generations. For each simulation, loci were filtered for minor allele frequency (MAF) > 0.01 for all analyses below. Filtering of the VCF files for MAF was done using *vcftools* (v0.1.16; [43]).

(b) Inversion polymorphisms

The inversion mutation rate per genome was drawn from the binomial distribution with a single draw and a probability of an inversion mutation of $\mu_{\text{inv}} = 0.001$, which equated to, on average, two inversions in the metapopulation per generation. This parameter is the estimated average genome-wide mutation rate that Berdan *et al.* [8] concluded in their review of species across different systems. The length of the inversion mutation was drawn from a discrete uniform distribution [100, 50 000]

(i.e. up to half the linkage group length) and the location was drawn randomly from the 20 linkage groups that were undergoing selection (inversions did not arise on the neutral linkage group). In inversion heterozygotes, crossovers in the inversion region were suppressed ($r = 0$); individuals homozygous for the inversion underwent recombination at rate r as usual. For computational simplicity, new inversions could not overlap within the same genome and could not break the end of a linkage group in the individual when they mutated (see electronic supplementary material, S3, figure S1). However, overlapping inversion windows (table 1) could evolve and segregate in the metapopulation (electronic supplementary material, S3, figure S1), and for this reason we neglected the dynamics of double crossovers or gene conversion due to computational intractability. However, our code appropriately modelled the inversion haplotypes that would be created by crossovers in homozygotes for the inverted arrangement (electronic supplementary material, S3, figure S2, see GitHub issue for thorough description: https://github.com/MesserLab/SLiM/issues/203). For each simulation, inversion mutations were filtered for MAF > 0.01.

(c) Control simulations

To evaluate how inversions facilitated adaptation, we needed two different control scenarios that were paired with every parameter combination's selection simulations (table 1). First, we carried out a paired no-inversion control simulation (table 1), which recorded how much LA would occur just based on the parameters of the simulation without inversion mutations (the null expectation for LA). The no-inversion control simulation was run using a separate random seed so mutations would not occur at the same position or time. Second, we carried out a no-selection control simulation (table 1) in which all individuals had equal fitness, but inversion mutations were allowed to occur (the null expectation for inversion dynamics by drift, mutation and migration). The no-selection control was run with the same seed to determine whether the same simulation without selection would result in a similar amount of divergence due solely to gene flow and drift. We used these two control simulations to create null distributions for various summary statistics described below.

(d) Q1: Under what conditions do inversions increase the degree of LA under gene flow?

To determine whether inversions influenced the degree of LA that occurred for each parameter combination, we compared simulations with $\mu_{inv} > 0$ to no-inversion control ($\mu_{inv} = 0$) simulations. LA was calculated as the sympatric versus allopatric contrast: the mean fitness of the sympatric demes (e.g. individuals in home/local deme) minus the mean fitness of allopatric demes (e.g. individuals in away/foreign deme; [44]).

(e) Identifying adaptive inversions for Q2–Q5

Before we could answer the other study questions, it was necessary to determine from our simulations *which* inversions were concentrating LA (i.e. divergence) above the level expected by chance. Using the paired control simulations, we identified adaptive inversion windows (table 1) as inversion windows that met three criteria. The first two criteria were met if the focal inversion window had a greater concentration of F_{ST} outliers in the inversion per unit map distance relative to collinear regions within the same genome. In the first criteria, outliers were QTNs with F_{ST} values as extreme or more extreme than the F_{ST} values of QTNs in no-selection simulations (this controlled for divergence expected by chance due to demography in the absence of selection). In the second criteria, outliers were QTNs with F_{ST} values as extreme or more extreme than the F_{ST} values for all neutral loci (on LG 21; this controlled for divergence expected by chance due to demography in the same simulation). The third criteria was met if the focal inversion window harboured a higher proportion of the total V_A than the collinear genome based on unit map distance (see electronic supplemenary material S2, section I.B. for details on all criteria). These three criteria were evaluated for all inversions that were present in the final generation of the simulation (i.e. generation 60 000). Inversions that met all three criteria were labelled as adaptive inversion windows and inversions that did not meet all three criteria were labelled as nonadaptive inversion windows (table 1). These criteria were not perfect, but were sufficient for interpreting the results.

(f) Q2: Under what conditions is divergence concentrated within inversions?

We evaluated the genomic architecture of divergence in all selection simulations where LA evolved. To identify when inversions were involved in divergence, we first identified simulations with a non-zero number of adaptive inversions that evolved. Then, we compared the amount of V_A that was present in the inverted segments of the genome to the expectation if V_A was evenly distributed across the 20 LGs (i.e. the percent of the genome that was inverted). This comparison allowed us to identify when V_A was concentrated in inverted regions above and beyond what would be expected.

(g) Q3: What are the characteristics of adaptive inversions?

For each parameter combination, we identified the average number of adaptive inversion windows, as well as their (i) length, (ii) age (i.e. based on the generation at which the inversion mutation arose), and (iii) the number of inversion window QTNs (table 1) scaled by the inversion length in cM. Data were compared across three categories: (i) for all adaptive inversion windows, (ii) for all nonadaptive inversion windows (may have contained some QTNs although they did not disproportionately contribute to LA), and (iii) for all no-selection inversion windows (table 1) from the paired control simulation.

In addition, we calculated the critical migration rate for each parameter combination following equation (3) of Yeaman and Whitlock (m_{crit}; [24]). The critical migration rate is the threshold migration rate below which locally favoured alleles tend to diverge between demes and persist for long enough to contribute to LA [24], and gives insight into whether individual QTNs would be swamping-prone or swamping-resistant based on their effect size. We visualized the distribution of QTNs effect sizes relative to the effect size above which they would be swamping-resistant (or below which they would be swamping-prone) across the following categories: (i) inside adaptive inversions, (ii) inside nonadaptive inversions, and (iii) in collinear regions.

(h) Q4: For an adaptive inversion to segregate and persist under local adaptation with gene flow, must it capture QTNs initially?

We assessed the genetic architecture that was captured when the inversion occurred (i.e. number and effect sizes of QTNs captured) and tracked how that genetic architecture evolved through time. To assess what an inversion captured at the time of mutation, we calculated the total effect size of the inversion haplotype, z_{inv} based on the sum of effect sizes at inversion haplotype

alleles (table 1) within the individual at the time of origin:

$$z_{\text{inv}} = \sum_{j=1}^{n_j} \sum_{k=1}^{2} \alpha_{jk} \tag{2.3}$$

where α_{jk} was the effect size of allele k at locus j and was summed across all n_j loci inside the inverted haplotype. Each adaptive inversion was labelled as either *neutral origin*, when $z_{\text{inv}} = 0$, or as *capture* when $z_{\text{inv}} \neq 0$ (i.e. absence or presence of QTNs inside the inverted arrangement when it mutated, respectively).

Once an inversion increased in frequency in the metapopulation, individuals could acquire different combinations of QTN alleles within that inverted arrangement, which would result in multiple inversion haplotypes (unique combinations of QTNs within the inverted arrangement among individuals) segregating in the metapopulation. For each inversion, we tracked the mean inversion effect size (table 1) by averaging z_{inv} across all copies of the inversion arrangement in the metapopulation every 1000 generations:

$$\bar{z}_{inv} = \frac{\sum_{c=1}^{n} \sum_{j=1}^{n_{cj}} \alpha_{cjk}}{n} \tag{2.4}$$

where α_{cjk} was the effect size of a given allele k at locus j in copy c of the focal inverted arrangement, n_{cj} was the number of QTNs in copy c, and n was the number of copies of the focal inverted arrangement. When like-signed alleles accumulated within the inverted arrangement (each potentially on different haplotypes), the mean inversion effect size grew in magnitude.

Next, at the end of the simulation, we evaluated whether the genomic region in which the inversion occurred gained QTNs over time (*gain* versus *no gain*). We evaluated this at the level of the metapopulation within the inversion window because QTN mutations that arose on the standard arrangement could still contribute to divergence. If the number of QTNs in the metapopulation within the inversion window at the time of origin and at the final time point were the same or fewer, adaptive inversions were labelled as 'no gain'; otherwise, they were labelled as 'gain'.

(i) Q5: Do outlier tests reliably detect adaptive inversions?

To test whether current genome scan methods correctly identified adaptive inversions, we ran all selection and no-selection control simulations through two commonly used outlier detection methods: (i) *OutFLANK*, which uses the F_{ST} distribution of neutral SNPs as a null distribution to identify putative loci under selection [45]; and (ii) *pcadapt*, which identifies outlier loci using principal components analysis that accounts for population structure (see electronic supplementary material, S2, section I.C.; [46]).

3. Results

To simplify the presentation of the results, we compared: (i) a polygenic architecture with a lower QTN mutation rate and moderate QTN effect sizes (QTNs typically swamping-resistant, except at high migration rates) to (ii) a highly polygenic architecture with a higher QTN mutation rate and small QTN effect sizes (QTNs typically swamping-prone, even at lower migration rates). Within the polygenic architecture, hundreds of loci (after MAF filtering) underlied the evolving trait with each QTN explaining on average 0.071% of the V_A (averaged across all parameter combinations and replicates; see electronic supplementary material, S3, figure S3 for breakdown of the distribution of QTN effect sizes and $\%V_A$ per parameter combination). Conversely, within the highly polygenic architecture, thousands of loci (after MAF filtering) underlied the diverging trait with each QTN only explaining on average 0.004% of the V_A (electronic supplementary material, S3, figure S3). A comparison of the amount of LA and the $\%V_A$ showed that results with and without environmental variance were similar; therefore, the data from the former were used for reporting the results (electronic supplementary material, S3, figures S4–S7).

(a) Overview

Most simulations reached a migration–mutation–drift equilibrium as evidenced by stability in the amount of LA over thousands of generations (electronic supplementary material, S3, figures S4 and S5). Over a large parameter space, simulations with inversions led to similar levels of LA as those without, and both had similar trajectories through time (electronic supplementary material, S3, figures S4 and S5). Although the simulations reached an equilibrium level of LA, in some cases there was an exchange of V_A from the collinear to the inverted genome through time that did not stabilize (electronic supplementary material, S3, figures S6 and S7). The ability of the metapopulation to reach an equilibrium level of LA while the underlying polygenic architectures never truly reached an equilibrium was possibly due to genetic redundancy leading to transient frequency changes and allelic covariances [26,29]. Interestingly, across many of our simulations where inversions were implicated in adaptation, multiple inversions evolved. In some cases, adaptive inversions were overlapping (electronic supplementary material, S3, figure S8*a*,*b*) or completely within other inversions (electronic supplementary material, S3, figure S8*c*,*d*). However, the latter case mainly occurred in the highly polygenic scenario.

(b) Q1: Under what conditions do inversions increase the degree of local adaptation under gene flow, and Q2: Under what conditions is divergence concentrated within inversions?

The genomic basis for LA varied both across different parameters and also between inversion and no-inversion control simulations. We binned the results into three different outcome categories depending on whether (i) divergence was concentrated within inversion window(s) (i.e. adaptive inversions were identified and V_A was concentrated within the inverted genome), and (ii) LA was higher in simulations with inversions compared to no-inversion control simulations (figure 1*a*,*b*). We observed transitions from one outcome to another outcome in some areas of the parameter space, and these were labelled with both outcomes.

(A) 'Outcome 1: Inversions do not concentrate divergence nor increase LA' (figure 1 red diamond outcome) occurred when inversion and no-inversion control simulations had similar levels of LA (figure 2*a–d*, red diamonds), and there was no concentration of divergence within inversions above that expected. This outcome commonly occurred under polygenic architectures, where alleles were typically swamping-resistant and the metapopulation quickly achieved an equilibrium level of LA (electronic supplementary material, S4, red diamond outcomes). These conditions generally did not result in a concentration of V_A within inversions more than expected

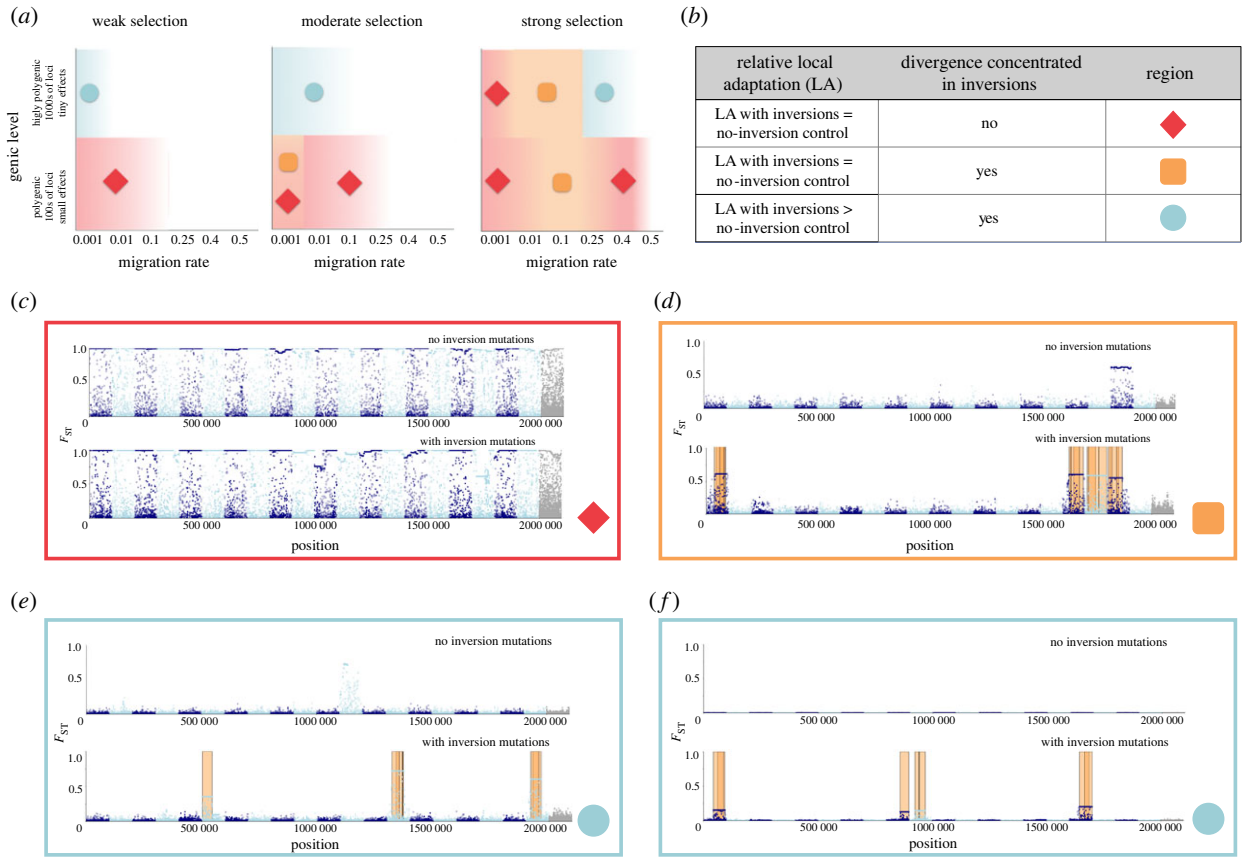

Figure 1. A description of the three conceptual outcomes that correspond to different genomic architectures that underlie trait divergence. (*a*) The conceptual outcome for each parameter combination. (*b*) Outcome definitions were based on: (i) the relative amount of local adaptation (LA) that evolves in inversion simulations relative to no-inversion control simulations, and (ii) whether divergence was concentrated in inversions. (*c–f*) Manhattan plots with no-inversion control example on top and with-inversion simulation on the bottom. Alternating light and dark blue represent different linkage groups, grey square points represent the neutrally evolving linkage group, and tan bars represent locally adaptive inversions present in the metapopulation. (*c*) Red diamond example (highly polygenic architecture, strong selection, and $m = 0.001$). (*d*) Orange square example (highly polygenic, strong selection, and $m = 0.1$) in which the degree of genomic clustering in no-inversion simulations was similar to those with inversions. (*e*) Blue circle example (highly polygenic, moderate selection, and $m = 0.001$) in which genomic clustering in no-inversion simulations was eroded by migration. (*f*) Blue circle example (highly polygenic, strong selection, and $m = 0.25$) in which no-inversion simulations did not evolve LA.

(figure 2*e,f*, red diamonds), nor the evolution of adaptive inversions (by our three criteria, figure 2*g,h* red diamonds).

For this outcome, the genetic architecture of adaptation varied from genome-wide divergence (figure 1*c* red diamond example, occurred under strong selection and low migration), to several loci of moderate effect (polygenic architectures with moderate/weak selection and low migration, or strong selection and high migration) in both inversion and no-inversion control simulations (see parameter combinations representing the red diamond outcome in electronic supplementary material, S4 for details). Under low gene flow and strong selection, divergence was typically genome-wide (with high F_{ST} across the genome) and there were rarely any inversions that were adaptive by our criteria. Under these low-gene flow conditions, however, there was a much larger number of inversions that established in the simulations with selection compared to the no-selection controls (electronic supplementary material, S4, pages 10 and 21). This suggested inversions were establishing at higher numbers than expected because they captured locally adapted sets of alleles after the deme had already reached an equilibrium level of LA, but this did not further affect the level of LA.

By contrast, this outcome still occurred under higher gene flow in the polygenic architectures, even though in these cases some proportion of QTNs were swamping-prone, and we might have expected inversions to offer an advantage (figure 1*a*, rightmost red diamond outcome in polygenic cases). In these cases, there was a lot more migration load (in the form of alleles that did not increase fitness in that deme) that made it unlikely that an inversion would harbour a favourable set of alleles at any point in time (see electronic supplementary material, S4, pages 5, 9). In most of the other cases, however, inversions were not necessary to facilitate adaptation in this parameter space because alleles were swamping-resistant.

Finally, some parameter combinations had variation between replicate simulations in whether adaptive inversions evolved or not. Adaptive inversions evolved in some replicates because inversions happened to occasionally capture an advantageous combination of already locally adapted alleles that had higher F_{ST} values than what would be expected due to drift (i.e. in comparison to loci on the neutral linkage group; see electronic supplementary material, S2, section I.B.4 criteria b for details). This transitory region of the parameter space was designated both a red diamond and an orange square (see below for orange square description).

(B) 'Outcome 2: Inversions concentrate divergence but do not increase LA' (figure 1; orange square outcome) occurred when divergence was concentrated in inversions more than

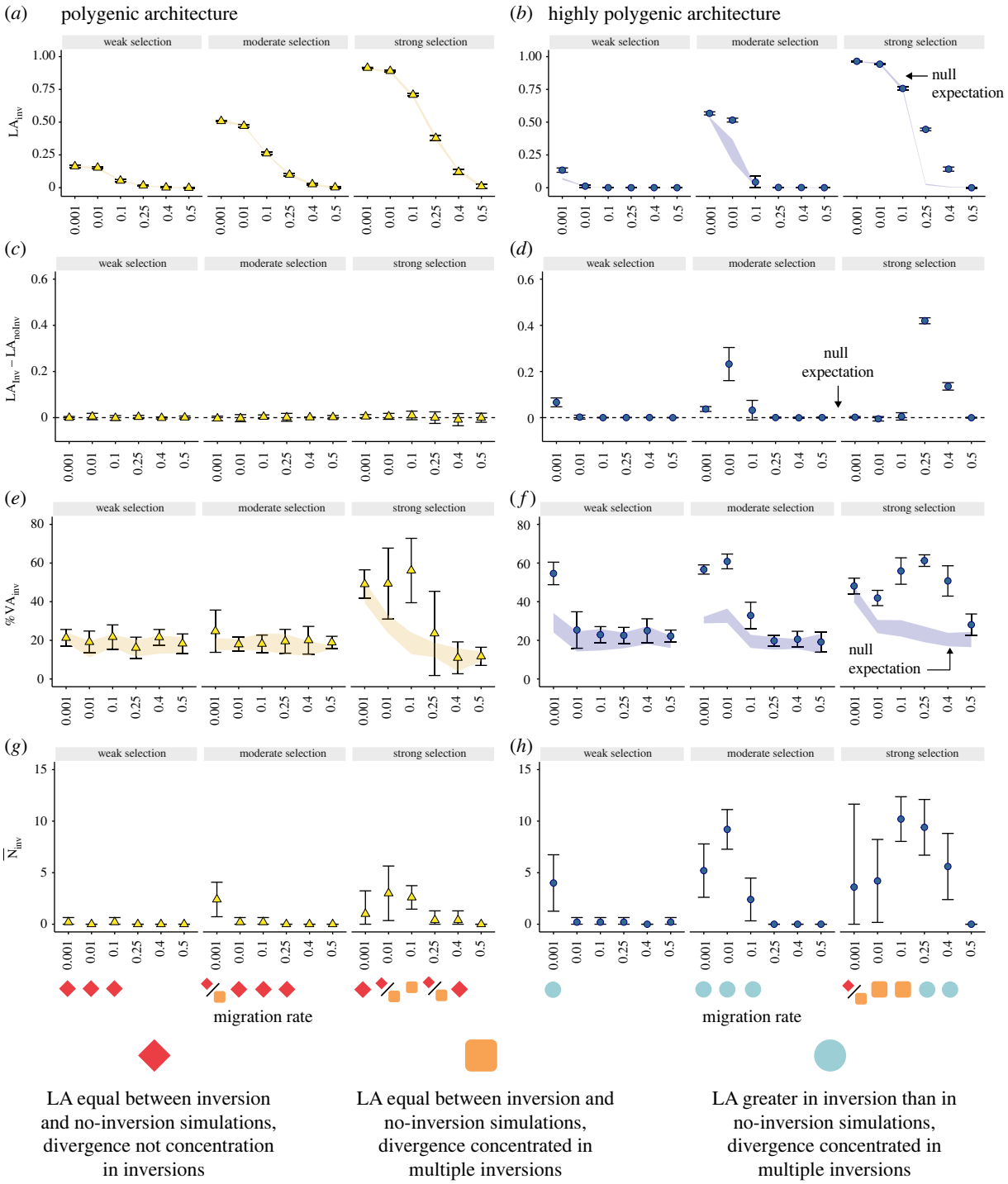

Figure 2. A summary of the local adaptation (LA), percent of additive genetic variance, and number of adaptive inversions that evolved across the parameter space. The left column is for the polygenic architecture and the right is for the highly polygenic architecture. (*a,b*) The average amount of LA that was reached in simulations that included inversions with results partitioned by migration rate (*x*-axis) and selection strength (panels within each plot). The ribbon represents the null expectation (average LA in the paired no-inversion control simulations ± 1 standard deviation (s.d.)). (*c,d*) The difference between the average LA reached in with-inversion simulations and paired no-inversion control simulation. The dashed line at zero represents the null (i.e. no difference between LA in inversion simulations and no-inversion simulations). (*e,f*) The percent of additive genetic variance found inside inverted regions. The ribbon represents the null expectation (the average percent of the genome that was inverted ± 1 s.d.). (*g,h*) The average number of resulting adaptive inversions ± 1 s.d. All averages and s.d. are across five replicate simulations. Outcome symbols for simulations with LA plotted on the x-axis at the bottom apply to all panels. All results are shown for simulations that included environmental variance.

expected, but inversions did not increase the amount of LA compared to no-inversion control simulations (figure 2*a–d*, orange squares). In this case, V_A was concentrated within inversion windows (figure 2*e,f*, orange squares), and multiple adaptive inversions typically evolved (figure 2*g,h*, orange squares).

This outcome could be achieved through three mechanisms. The first mechanism occurred with polygenic architectures at (i) low migration and moderate selection and (ii) intermediate migration rates and strong selection (figure 1*a*, red diamond/orange square outcomes) when QTN alleles were not swamping-prone. Under these conditions, adaptive inversions typically established long after LA was achieved in the metapopulation (e.g. younger inversions) because they tended to capture locally adapted sets of

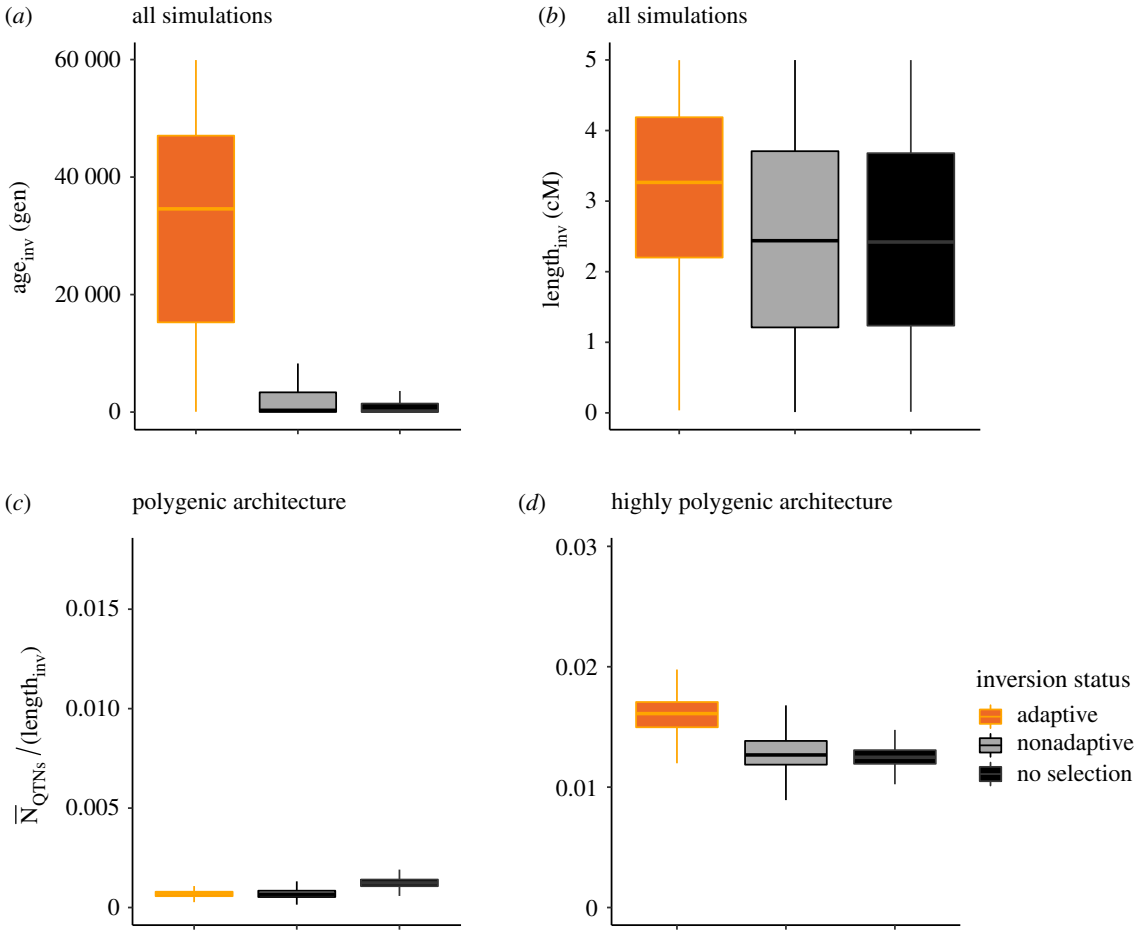

Figure 3. The distribution of three inversion characteristics across all simulations. (*a*) Inversion age in generations (gen). (*b*) Inversion length in centimorgans (cM). (*c*,*d*) The average number of inversion quantitative trait nucleotides (QTNs) scaled by the total length of the inversion for (*c*) polygenic and (*d*) highly polygenic architectures. In selection simulations, divergence was concentrated in adaptive inversions and not concentrated in nonadaptive inversions. Inversions from the no-selection control simulations indicate the expected characteristics from demography. All results are shown for simulations that included environmental variance.

alleles (electronic supplementary material, S4, pages 6, 11–14). The capture event(s) did not lead to a higher level of LA compared to no-inversion controls, due to alleles not being prone to swamping in the latter.

The second mechanism occurred with highly polygenic architectures at low/moderate migration and under strong selection (figure 1*a* orange square outcome in highly polygenic architectures, strong selection, $m = 0.01$), when QTNs were a combination of swamping-prone and swamping-resistant (electronic supplementary material, S4, page 22). In simulations with inversions, adaptive inversions typically arose early in adaptation and gained swamping-prone QTNs through time, leading to concentration of QTNs within the inversion (electronic supplementary material, S4, page 22). The simulations without inversions achieved similar levels of LA, due to many swamping-resistant QTNs scattered across the genome (electronic supplementary material, S4, page 22).

The third mechanism also occurred with highly polygenic architectures under strong selection, but with higher levels of migration (figure 1*a* second orange square in highly polygenic architectures, strong selection, $m = 0.1$), when many QTN mutations were swamping-prone. In this case, migration was high enough such that genomic clustering (table 1) in the no-inversion control simulations was necessary for alleles to avoid swamping by migration, but not so high as to erode genomic clustering (e.g. figure 1*d* orange square; electronic supplementary material, S4, page 23). Thus, simulations with and without inversions achieved similar levels of LA due to genomic clustering. Without inversions, clustering produced similar patterns to an adaptive inversion in F_{ST} outlier plots and genotype heatmaps (e.g. electronic supplementary material, S3, figure S9). In the simulations with inversions (and in contrast to the first mechanism discussed above), adaptive inversions typically arose early in adaptation and gained QTNs through time (electronic supplementary material, S4, page 23).

(C) 'Outcome 3: Inversions concentrate divergence and increase LA' (figure 1; blue circle outcome) occurred when divergence was concentrated in inversions more than expected based on their size, and inversions also increased the amount of LA compared to no-inversion control simulations (figure 2*b*,*d*, blue circles). The V_A was concentrated within inversion windows above that expected based on their size (figure 2*f*, blue circles) and genomes harboured multiple adaptive inversions (figure 2*h*, blue circles). This only occurred under highly polygenic scenarios, when a large proportion or all QTN mutations were swamping-prone ($m_{crit} >> m$, electronic supplementary material, S4, pages 17–20, 24–25). Under high migration, no-inversion control simulations did not form genomic clustering because the clusters were partially or fully eroded by migration (figure 1*e* blue circle outcome), and thus simulations with inversions achieved a higher level of LA (electronic supplementary material, S4, pages 24–25). When migration was low and selection was weak/moderate, only a slight or modest increase in LA was achieved by the addition of inversions (electronic supplementary material, S4, pages 17–20).

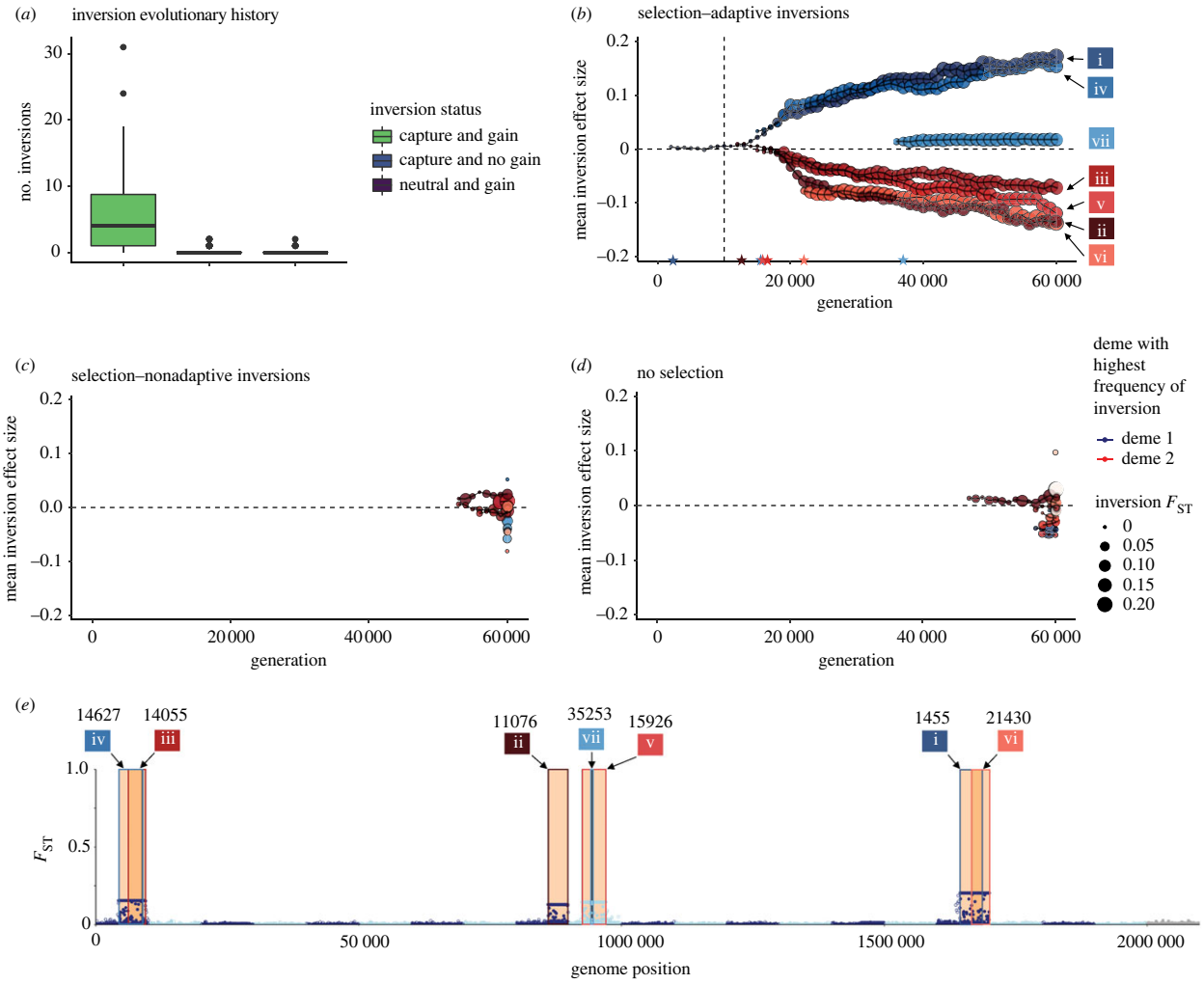

Figure 4. A summary of the origin dynamics of inversions. (*a*) The number of adaptive inversions belonging to each of three possible categories of capture and/or gain. (*b–d*) An example simulation (highly polygenic architecture, strong selection, $m = 0.25$) highlighting the dynamics of capture and gain. The mean inversion effect size on the phenotype is plotted through time for (*b*) all adaptive inversions, (*c*) all nonadaptive inversions and (*d*) inversions from the paired no-selection control simulation. Each track line is an inversion with the seven adaptive inversions labelled as *i–vii* (see main text for more details on the origin dynamics of each of these inversions). Colours represent which deme the inverted arrangement is at a higher frequency in (deme 1 in blue and deme 2 in red with phenotypic optimums at +1 or −1, respectively) with coloured stars on the *x*-axis marking the generation the corresponding inversion arose. Bubble size is the F_{ST} value for the inversion at each time step. (*e*) Manhattan plot corresponding to the same example simulation with labels *i–vii* above each inversion colour coded to match labels in (*b*) with the generation of origin for each inversion listed above the inversion labels.

Across all blue circle outcomes, adaptive inversions typically arose early in adaptation and gained QTNs through time (electronic supplementary material, S4, pages 17–20, 24–25; see also Q4 below).

(D) Outcome 4: No LA. Under high gene flow and weak-to-moderate selection, LA did not evolve (blank space; figure 1*a*). In a few rare cases, very few adaptive inversions evolved, even though no LA occurred (figure 2*g*,*h*; see parameters that have no symbol on *x*-axis, but have some number of adaptive inversions). This meant that the inversions harboured divergence for the trait above what was expected by random, but not enough to contribute to divergence under high gene flow.

(c) Q3: What are the characteristics of adaptive inversions?

Across all simulations where adaptive inversions evolved, we found that these inversions tended to be older (figure 3*a*) and longer (figure 3*b*). Additionally, they contained more length-normalized QTNs when highly polygenic, but not when polygenic compared to nonadaptive inversions and neutral inversions from the no-selection paired control simulation (figure 3*c*,*d*). There were some exceptions to these general patterns based on the conditions of the simulation (but see electronic supplementary material, S3, figure S10 for breakdown of characteristics across the parameter space). For instance, sometimes inversions arose late in adaptation and captured locally adapted alleles. This occurred when QTNs were a combination of swamping-prone and swamping-resistant (as described 'Inversions concentrate divergence but do not increase LA'), or when a recent inversion mutation overlapped with an older adaptive inversion.

(d) Q4: For an adaptive inversion to segregate and persist under local adaptation with gene flow, must it capture QTNs initially?

Three distinct evolutionary histories for adaptive inversions were evaluated: (i) *neutral and gain*: QTNs were absent within inversions at the time of origin, but accumulated over time; (ii) *capture and no gain*: at the time of mutation

the inversion captured one or more QTNs, but did not gain additional QTNs through time; and (iii) *capture and gain*: at the time of mutation the inversion captured one or more QTNs and also gained additional QTNs over time. Across all simulations that had adaptive inversions, we found that the overwhelming majority arose by capturing standing genetic variation at the time of mutation and then accumulating mutations through time (i.e. capture and gain; figure 4*a*). It was not straightforward to determine the relative importance of capture versus gain to inversion evolution, but we could understand the qualitative contribution of each by examining the dynamics of individual inversions.

We illustrate this with a simulation from the highly polygenic architecture, high gene flow scenario (strong selection, $m = 0.25$, blue circle; figure 4*b–e*), in which simulations with inversions achieved LA while those without inversions did not. All inversions discussed and shown are those that were present in the final generation of the simulation (i.e. 60 000). This simulation evolved seven adaptive inversions that were numbered according to when they arose (*i–vii*). In this simulation, one inversion arose before the burn-in and, by drift, had a small positive effect on the phenotype at the onset of selection (inversion *i*), which set it on a trajectory to gain mean inversion effect size through time (figure 4*b*). After the onset of selection, four more inversions (*ii–v*) captured a small set of locally adapted alleles and then gained mean inversion effect size and F_{ST} through time (figure 4*b*; electronic supplementary material, S3, figure S11). The age distribution of QTNs within these first five inversions shows that the majority of QTNs were gained through time (electronic supplementary material, S3, figure S12*a*,*b*). In addition, inversions *ii–v* established during a bout of adaptation (15 000–20 000 generations). By contrast, two inversions (*vi–vii*) arose after LA had reached equilibrium, primarily captured diverged QTNs already present in the genome (electronic supplementary material, S3, figure S12*a*, *b*), and did not change much in mean inversion effect size through time (figure 4*b*). Their establishment did not increase the total amount of LA (electronic supplementary material, S4, page 24). Interestingly, there was considerable mutation load (in terms of alleles that bring the phenotype away from the optimum) segregating inside all the inversions (electronic supplementary material, S3, figure S13).

Nonadaptive inversions and control inversions (from no-selection simulations) segregating at the end of the simulation typically arose recently (figure 4*c*,*d* respectively), had low F_{ST} values (electronic supplementary material, S3, figure S11), and consisted of QTNs that were 2–3 orders of magnitude younger than QTNs in adaptive inversions (electronic supplementary material, S3, figure S12*c*,*d*). Although the amount of LA reached an equilibrium after the initial adaptive inversions established early in divergence, the mean inversion effect size (figure 4*b*) and inversion F_{ST} (electronic supplementary material, S3, figure S11) steadily increased through time and did not appear to reach equilibrium. This suggested a gradual transition of the genetic architecture of divergence from the collinear genome to the inverted genome through time. Other inversions arose throughout the simulation, but were lost due to either drift or swamping.

Three sets of inverted arrangements evolved that overlapped on the genetic map (electronic supplementary material, S3, figure S1). These overlapping inverted arrangements appeared as a single large inversion block in both F_{ST} outlier plots and genotype heatmaps (electronic supplementary material, S3, figure S9). The first overlap consisted of inversion arrangements *i* and *vi* (figure 4*e*): inversion *i* established first in deme 1 (blue colour; figure 4*b*), followed by inversion *vi* several thousand generations later. However, inversion *vi* was at a higher frequency in deme 2 (i.e. red colour; figure 4*b*) because it captured alleles on the standard arrangement that had already diverged due to being within the inversion *i* window. The second overlap of inversion arrangements were *iii* and *iv* (figure 4*e*), which established one shortly after the other in a bout of adaptation (electronic supplementary material, S3, figure S11), but again each arrangement was at a higher frequency in an opposite deme (figure 4*b*). Finally, the third overlap consisted of inversion arrangements *v* and *vii* (figure 4*e*), where *v* established early in divergence in deme 2 (i.e. red colour; figure 4*b*) and inversion *vii* arose within the bounds of inversion *v* and established late in divergence in deme 1 (i.e. blue colour; figure 4*b*). Inversion *vii* captured locally adapted alleles and its mean inversion effect size remained constant (figure 4*b*), and thus did not affect the level of LA. There was one other inversion (inversion *ii*) that established in deme 2 during the bout of adaptation (i.e. red colour; figure 4*b*), but did not overlap with another inversion.

(e) Q5: Do outlier tests reliably detect adaptive inversions?

Overall, we found that *pcadapt* and *OutFLANK* accurately categorized adaptive, nonadaptive, and neutral inversions as outliers for genetic differentiation across a wide parameter space (electronic supplementary material, S3, figure S14*a–d*; compare blue bars to yellow). Although both methods were generally accurate, each had slight, unique weaknesses when differentiating between adaptive and nonadaptive inversions (see electronic supplementary material, S3, figures S14–S16 for detailed explanations and examples of weaknesses).

4. Discussion

Understanding the conditions in which inversion polymorphisms not only harbour loci affecting adaptive divergence but actually increase the amount of LA that populations can reach is an important yet unresolved evolutionary question. Using simulations that both incorporate flexible inversion characteristics and combine quantitative and population genetic frameworks, our study unites these two fields and provides a unique perspective on the way inversion polymorphisms influence genome architecture and LA. We showed that inversions facilitated LA under high gene flow when loci were mostly swamping-prone, spatially divergent selection on the phenotype (determined by the strength of stabilizing selection on the trait and the difference in trait optimums among demes) was sufficiently strong, and the trait was governed by a highly polygenic architecture (i.e. high mutation rate, small mutation effect size on the trait). Under these conditions, genomes with multiple long, old inversions evolved, and each inversion acted similarly to a supergene complex of loci. In addition, inversions also facilitated adaptation at low migration and weak-to-moderate selection, but to a much lesser degree. In addition, we showed that inversions could still harbour the genetic

basis of LA, even when they did not facilitate a higher level of LA.

Additionally, we found that the degree to which alleles were prone to swamping by migration indicated whether inversions facilitated LA. When a major proportion of alleles were swamping-prone, divergence was often concentrated within inversions. As the proportion of swamping-prone alleles increased, the amount of divergence in inversions typically increased. There was an exception to this general rule: we found that in a few cases adaptive inversions did not evolve when alleles were swamping-prone. This outcome occurred when there was more migration load (in the form of alleles segregating in a deme that did not increase fitness in that deme) and mutations of larger phenotypic effects, which made it rare that an inversion would harbour a favourable set of alleles at any point in time. On the other hand, when the majority of mutations were swamping-resistant, inversions rarely concentrated divergence more than expected. Occasionally they would capture a beneficial combination of alleles that were already diverged and therefore, would not influence the total amount of LA. These general patterns may be hard to test empirically, but are important avenues for the development of future theory.

(a) Genetic architecture of local adaptation

By contrast to previous models that focused on the capture of advantageous alleles by inversions (which typically arises after a period of allopatry), our research showed that the evolution of adaptive inversions did not require these conditions and could occur with high gene flow. However, adaptive inversions could arise in a variety of ways which was affected by not only the level of gene flow, but also the degree of spatially divergent selection. Together these processes, along with the strength of genetic drift, determined the extent to which individual QTNs were swamping-prone and the conditions when inversions were beneficial for adaptation.

Although the role of selection and its interplay with both migration and the genomic architecture underlying divergence has not been fully resolved in the literature [47,48], many empirical examples of ecotype divergence have found that genomic clustering and inversions underlie differentiation [10,11,49]. A growing body of theory has supported these empirical findings [24,32,50], although previous models have not compared the dynamics of genomic clustering to that of inversions in a common modelling framework, as we have here. By comparing inversion simulations to no-inversion-control simulations, we highlighted how the genomic architecture of adaptation was influenced by the level of swamping. When most alleles were swamping-resistant, we did not find that genomic clustering or inversions played a major role in adaptation. As the proportion of swamping-prone alleles increased (either due to decreasing selection strength and/or increasing migration), genomic clustering in no-inversion simulations resulted in LA equal to that of genomes with inversion mutations under a narrow range of conditions (i.e. strong selection and intermediate migration, $m = 0.1$). As the proportion of swamping-prone alleles increased further (either due to decreasing selection strength and/or increasing migration), inversion simulations achieved a higher level of LA than no-inversion simulations due to genomic clustering being partially (moderate selection, $m = 0.01$) or fully (strong selection, $m = 0.25$ and 0.4) eroded by swamping in the latter.

Some empirical studies have distilled the relationship between genetic architecture and gene flow to a simple relationship: as gene flow increases, more clustering evolves. We showed that it is a much more nuanced story when the strength of selection on both the trait and the individual QTNs were considered, as these greatly influence the degree of swamping. In addition, we showed that when most loci were swamping-prone, genomic clustering was eroded and inversions were the only mechanism that facilitated adaptation. Determining the exact threshold in which genomic clustering is eroded and inversions are the only mechanism by which adaptation can occur is an important next step for analytical theory. Additionally, quantifying critical migration rates and the degree to which genomic architectures are swamping-prone is an important step for future empirical research.

When inversions are implicated in adaptation, they are often outliers in genome scan methods and this can lead investigators to focus entirely on the inversion region. However, our simulations showed that these outliers can consist of many polygenic loci with small effects [24], without any large effect loci affecting the trait. By simulating a quantitative genetic trait, we were able to partition additive genetic variance (V_A) into different regions of the genome. Under conditions in which inversions played an important role in adaptation, inversions rarely explained more than 50–60% of the V_A. Thus, our simulations predict that if inversions evolve under highly polygenic architectures, a substantial part of the V_A will be outside of inversions; however, it will remain undetectable by genome scans because the trait is governed by loci of small effect. In line with this prediction, a recent empirical study that partitioned V_A for adaptive traits in the marine snail *Littorina saxatilis* found that approximately half of the V_A was inside inversions and half in the collinear genome [51]. Although it is tempting to want to identify targets of selection that may be harboured in inversions, care must be taken when interpreting potential targets of selection inside inversions and empirical studies should consider how a polygenic trait architecture may influence those interpretations.

(b) Capture versus accumulation and inversion length and age

There is currently a debate about whether inversions capture QTNs at the time of mutation or if they arise neutrally and accumulate QTNs through time. Some have suggested that the accumulation of mutations inside the inversion over time caused it to establish and persist (e.g. gain scenario; [12]). Conversely, in species where ecotype differentiation predates the inversion age estimates, researchers have speculated that the inversion captured locally adapted alleles at the time of mutation (e.g. capture scenario; [11]). Across nearly all of our simulations, the most common mechanism for the establishment of adaptive inversions was capture combined with accumulation/gain. Although we were unable to quantify the relative importance of capture and gain, we were able to qualitatively determine whether the dynamics were driven by mostly capture or mostly gain. Under conditions where alleles were not swamping-prone (e.g. low gene flow) inversions were rarely involved in adaptation; but when inversions were involved, they were typically young and

captured alleles that were already locally adapted, followed by little accumulation.

In contrast, under conditions where alleles were swamping-prone, inversions typically arose early in adaptation and captured a small number of advantageous like-effect alleles (which allowed the inversion to overcome drift), followed by a substantial accumulation of QTNs in the inversion window until migration–drift–selection equilibrium was reached. This resulted in most adaptive inversions being much larger and older compared to nonadaptive inversions. A larger size increased the probability of capturing an advantageous combination of loci that pushed them over the drift threshold early in adaptation, and over thousands of generations they gained mutations that caused adaptive divergence. Under these swamping-prone conditions, large inversions were unlikely to establish after the phenotype reached equilibrium for that deme because they would be more likely to capture an unfavourable combination of alleles that caused the phenotype to move away from that equilibrium and potentially overshoot the optimum. Capture-and-gain could be a plausible mechanism to explain the old age and large size of inversions in empirical studies [3,11].

On the other hand, we did observe overlapping inversions or inversions-within-inversion mutations arising after the phenotype reached equilibrium in swamping-prone simulations; a phenomenon that has been observed empirically in LA (e.g. [13,38,39]). The overlapping inversions arose later in the simulation because they captured QTNs that were already locally adapted within an inversion that arose early in the simulation via a capture-a-little-and-gain-a-lot mechanism. Often the newer overlapping inversion would capture locally adapted alleles on the standard arrangement in the opposite deme as the one with the higher frequency of the inverted arrangement.

Taken together, our findings lend support to a stepwise model of supergene evolution where adaptation occurs via multiple structural changes and accumulation of 100s of linked loci underlying an evolving trait [52,53]. Note that the way our simulations were set up, in which a large amount of V_A was segregating at the onset of environmental change, is partly why capture and gain/accumulation was so commonly observed. Nevertheless, these results highlight an unexplored dynamic in empirical studies and show that the capture and gain of very small effect alleles is a plausible mechanism for adaptive inversions to arise.

5. Future directions

Although our simulations incorporated many aspects of realism previously lacking in other modelling studies, there are still other mechanisms important for the evolution of inversions in adaptation that we did not address. These include mechanisms that may hinder the spread and maintenance of an inversion, such as the accumulation of globally deleterious mutations within inverted regions [8]. Note that in our model, new QTN mutations could behave as locally deleterious because their effect on fitness depended on the genetic background on which they arose. Therefore, in our simulations the genetic background of an individual could greatly influence whether a new inversion established or was lost. True globally deleterious mutations, however, can also generate overdominance (i.e. heterozygote advantage) which does not generally happen for LA alleles except under special conditions (e.g. fluctuating environments). This could lead to different dynamics than our LA alleles. Inclusion of true deleterious mutations was not explored in our simulations, but would be an important avenue for future research to understand the interaction of deleterious mutations and LA alleles on the invasion and maintenance of inversions.

Gene flux can also decrease the establishment probability of an inversion through the breakup of adaptive loci via gene conversion or double-crossover events [34,54]. Rates of gene flux have mainly been estimated in *Drosophila* and have ranged in value between approximately 10^{-5} to 10^{-8} [55]. Previous models have found that the inclusion of gene flux can reduce the establishment probability of an inversion [20,34]. These studies, however, assumed conditions in which the genetic material that 'fluxed' was perfectly adapted to its local conditions, as well as an oligogenic architecture with only a few loci underlying adaptation [20,34]. Although gene flux was not simulated in this study because it was computationally intractable, the influence of gene flux on our results is not immediately clear. Due to the polygenic nature of our simulations and genotypic redundancy, small-effect alleles with both positive and negative effects on the phenotype segregated within inversions (a type of mutation load; [26,29]). This demonstrates that adaptive inversions can have, at any point in time, both a favourable and an unfavourable set of alleles for the local conditions. Gene flux would thus deliver alleles of both effect sizes to the other orientation, which may not be as detrimental to LA as it would be if all alleles within the inversion were perfectly adapted to their local conditions.

On the other hand, we also showed in our simulations that inversions facilitated adaptation even without consideration of additional mechanisms that, although possibly hindering the initial spread of an inversion, may also facilitate increased divergence of an already established inversion. A few examples include heterozygote disadvantage through underdominance (e.g. decreased fecundity due to unbalanced gametes; [6,56,57]) or genomic incompatibilities (e.g. Bateson-Dobzhansky-Müller incompatibilities; [8,58–60]). Other mechanisms, such as shifting genes to a new regulatory region or through disrupting sequences in the inversion breakpoints, may increase or decrease the establishment probability of inversions depending on their phenotypic effects. These mechanisms would involve simulating selection on the inversion arrangement itself, which is different from our simulations in which selection acted directly on the inversion content (e.g. QTNs) and indirectly on the arrangement. In addition, we did not simulate conditions to evaluate linked selection (e.g. background selection or selective sweeps of neutral loci). These considerations are important next steps for understanding the complex dynamics of inversions in adaptation.

Future research could seek to relax additional assumptions made in this study. Firstly, our simulations were run for 60 000 generations (30 N) and thus represent the amount of LA and genetic architecture present at a snapshot in time. Although most simulations reached an equilibrium amount of LA, in some cases we observed a gradual shift of V_A from the collinear genome to the inverted genome that did not seem to reach equilibrium. Secondly, lower heritabilities than evolved here (either due to higher environmental noise or lower V_A) may lessen the probability of inversions being involved in adaptation. Investigating the equilibrium dynamics over greater time scales and lower heritabilities is an important direction for future research.

6. Conclusion

Our results highlight how highly polygenic architectures can lead to an inversion behaving as a single large-effect locus. Previous theory has shown that an inversion does not offer a selective advantage for closely linked loci because they are effectively swamping-resistant [23], and our results corroborate this theory. When loci are loosely linked and swamping-prone, however, the advantage of being captured by an inversion is much greater and this increases the establishment probability of the inversion [23]. In other words, large-effect loci (that are not swamped by gene flow) do not need to be captured by an inversion to lead to LA, while under polygenicity there are many more possible locations for useful inversions, making the probability of an adaptive inversion to arise much higher. Exceptions might be in an allopatric model (such as [22]), whereby an inversion that arises in allopatry and captures like-effect loci will persist under secondary contact, or in some of the scenarios presented here, in which an inversion captures locally adapted alleles, but do not lead to higher levels of LA.

In conclusion, our simulations raise interesting hypotheses that could be tested empirically. When inversions are inferred to play a central role in adaptive divergence of a trait under high gene flow, our simulations predict that the trait will be highly polygenic (H1). This hypothesis can now be tested by using gene editing to 'flip' an inverted arrangement back to a standard arrangement and then conducting quantitative trait mapping. Our simulations also predict that inversions will play a central role when most QTNs are swamping-prone, while the phenotype is under strong spatially divergent selection (H2). Determining the extent to which alleles underlying a quantitative trait are swamping-prone (which is determined by migration rate, drift, and the strength of selection) is an important direction for future research. Our simulations also predict that adaptive inversions will harbour a significant proportion of the V_A in the trait, but a significant proportion will also be harboured outside adaptive inversions (H3). This hypothesis can be tested by partitioning the V_A to inverted and collinear regions with an animal model (see [51] for an example). Furthermore, with sequencing data now being used to identify all inversions segregating in a metapopulation (e.g. [13,61]), the predictions from this study regarding the characteristics for adaptive versus nonadaptive inversions (e.g. size, age) can be tested (H4). Research aimed at evaluating these predictions will have important implications for advancing our understanding of how intraspecific diversity evolves in the face of gene flow.

Data accessibility. All code and simulation outputs are available from the Dryad Digital Repository: https://doi.org/10.5061/dryad.mkkwh712q [62].

Authors' contributions. S.M.S.: conceptualization, data curation, formal analysis, methodology, visualization, writing—original draft, writing—review and editing; B.C.H.: methodology, writing—review; K.E.L.: conceptualization, funding acquisition, supervision, writing—review and editing.

All authors gave final approval for publication and agreed to be held accountable for the work performed therein.

Conflict of interest declaration. We declare we have no competing interests.

Funding. We acknowledge funding from the National Science Foundation award no. 1655701.

Acknowledgements. We would like to thank the editor Emma Berdan, Jeff Feder, anonymous reviewers, Molly Albecker, Thais Bittar, Alan Downey-Wall, Áki Láruson, Dylan Titmuss, Luke Abbatessa and Jonathan Grabowski for helpful feedback on earlier manuscript drafts and analyses. We would like to thank Vince Buffalo, Andrew Kern and Peter Ralph for helpful discussions and collaborative coding which led to the accurate simulation of inversions.

References

1. Richardson JL, Urban MC, Bolnick DI, Skelly DK. 2014 Microgeographic adaptation and the spatial scale of evolution. *Trends Ecol. Evol.* **29**, 165–176. (doi:10.1016/j.tree.2014.01.002)
2. Tigano A, Friesen VL. 2016 Genomics of local adaptation with gene flow. *Mol. Ecol.* **25**, 2144–2164. (doi:10.1111/mec.13606)
3. Wellenreuther M, Bernatchez L. 2018 Eco-evolutionary genomics of chromosomal inversions. *Trends Ecol. Evol.* **33**, 427–440. (doi:10.1016/j.tree.2018.04.002)
4. Faria R, Johannesson K, Butlin RK, Westram AM. 2019 Evolving inversions. *Trends Ecol. Evol.* **34**, 239–248. (doi:10.1016/j.tree.2018.12.005)
5. Wellenreuther M, Mérot C, Berdan E, Bernatchez L. 2019 Going beyond SNPs: the role of structural genomic variants in adaptive evolution and species diversification. *Mol. Ecol.* **28**, 1203–1209. (doi:10.1111/mec.15066)
6. Kirkpatrick M. 2010 How and why chromosome inversions evolve. *PLoS Biol.* **8**, e1000501. (doi:10.1371/journal.pbio.1000501)
7. Fuller ZL, Koury SA, Phadnis N, Schaeffer SW. 2019 How chromosomal rearrangements shape adaptation and speciation: case studies in *Drosophila pseudoobscura* and its sibling species *Drosophila persimilis*. *Mol. Ecol.* **28**, 1283–1301. (doi:10.1111/mec.14923)
8. Berdan EL, Blanckaert A, Butlin RK, Bank C. 2021 Deleterious mutation accumulation and the long-term fate of chromosomal inversions. *PLoS Genet.* **17**, e1009411. (doi:10.1371/journal.pgen.1009411)
9. Wang J, Wurm Y, Nipitwattanaphon M, Riba-Grognuz O, Huang Y-C, Shoemaker D, Keller L. 2013 A Y-like social chromosome causes alternative colony organization in fire ants. *Nature* **493**, 664–668. (doi:10.1038/nature11832)
10. Twyford AD, Friedman J. 2015 Adaptive divergence in the monkey flower *Mimulus guttatus* is maintained by a chromosomal inversion. *Evolution* **69**, 1476–1486. (doi:10.1111/evo.12663)
11. Kirubakaran TG *et al*. 2016 Two adjacent inversions maintain genomic differentiation between migratory and stationary ecotypes of Atlantic cod. *Mol. Ecol.* **25**, 2130–2143. (doi:10.1111/mec.13592)
12. Lamichhaney S *et al*. 2016 Structural genomic changes underlie alternative reproductive strategies in the ruff (*Philomachus pugnax*). *Nat. Genet.* **48**, 84–88. (doi:10.1038/ng.3430)
13. Faria R *et al*. 2019 Multiple chromosomal rearrangements in a hybrid zone between *Littorina saxatilis* ecotypes. *Mol. Ecol.* **28**, 1375–1393. (doi:10.1111/mec.14972)
14. Arostegui MC, Quinn TP, Seeb LW, Seeb JE, McKinney GJ. 2019 Retention of a chromosomal inversion from an anadromous ancestor provides the genetic basis for alternative freshwater ecotypes in rainbow trout. *Mol. Ecol.* **28**, 1412–1427. (doi:10.1111/mec.15037)
15. Lucek K, Gompert Z, Nosil P. 2019 The role of structural genomic variants in population differentiation and ecotype formation in *Timema cristinae* walking sticks. *Mol. Ecol.* **28**, 1224–1237. (doi:10.1111/mec.15016)
16. Huang K, Andrew RL, Owens GL, Ostevik KL, Rieseberg LH. 2020 Multiple chromosomal inversions contribute to adaptive divergence of a dune sunflower ecotype. *Mol. Ecol.* **29**, 2535–2549. (doi:10.1111/mec.15428)

17. Lotterhos KE. 2019 The effect of neutral recombination variation on genome scans for selection. *Genes Genomes Genet.* **9**, 1851–1867. (doi:10.1534/g3.119.400088)
18. Booker TR, Yeaman S, Whitlock MC. 2020 Variation in recombination rate affects detection of outliers in genome scans under neutrality. *Mol. Ecol.* **29**, 4274–4279. (doi:10.1111/mec.15501)
19. Kirkpatrick M, Barton N. 2006 Chromosome inversions, local adaptation and speciation. *Genetics* **173**, 419–434. (doi:10.1534/genetics.105.047985)
20. Feder JL, Gejji R, Powell THQ, Nosil P. 2011 Adaptive chromosomal divergence driven by mixed geographic mode of evolution. *Evolution* **65**, 2157–2170. (doi:10.1111/j.1558-5646.2011.01321.x)
21. Guerrero RF, Rousset F, Kirkpatrick M. 2012 Coalescent patterns for chromosomal inversions in divergent populations. *Phil. Trans. R. Soc. B* **367**, 430–438. (doi:10.1098/rstb.2011.0246)
22. Feder JL, Nosil P, Flaxman SM. 2014 Assessing when chromosomal rearrangements affect the dynamics of speciation: implications from computer simulations. *Front. Genet.* **5**, 295. (doi:10.3389/fgene.2014.00295)
23. Charlesworth B, Barton NH. 2018 The spread of an inversion with migration and selection. *Genetics* **208**, 377–382. (doi:10.1534/genetics.117.300426)
24. Yeaman S, Whitlock MC. 2011 The genetic architecture of adaptation under migration-selection balance. *Evolution* **65**, 1897–1911. (doi:10.1111/j.1558-5646.2011.01269.x)
25. Lenormand T. 2002 Gene flow and the limits to natural selection. *Trends Ecol. Evol.* **17**, 183–189. (doi:10.1016/S0169-5347(02)02497-7)
26. Yeaman S. 2015 Local adaptation by alleles of small effect. *Am. Nat.* **186**, S74–S89. (doi:10.1086/682405)
27. Lowry DB, Willis JH. 2010 A widespread chromosomal inversion polymorphism contributes to a major life-history transition, local adaptation, and reproductive isolation. *PLoS Biol.* **8**, e1000500. (doi:10.1371/journal.pbio.1000500)
28. Flaxman SM, Wacholder AC, Feder JL, Nosil P. 2014 Theoretical models of the influence of genomic architecture on the dynamics of speciation. *Mol. Ecol.* **23**, 4074–4088. (doi:10.1111/mec.12750)
29. Láruson ÁJ, Yeaman S, Lotterhos KE. 2020 The importance of genetic redundancy in evolution. *Trends Ecol. Evol.* **35**, 809–822. (doi:10.1016/j.tree.2020.04.009)
30. Shi Y, Bouska KL, McKinney GJ, Dokai W, Bartels A, McPhee MV, Larson WA. 2021 Gene flow influences the genomic architecture of local adaptation in six riverine fish species. *Mol. Ecol.* (doi:10.1111/mec.16317)
31. Connallon T, Olito C. 2021 Natural selection and the distribution of chromosomal inversion lengths. *Mol. Ecol.* (doi:10.1111/mec.16091)
32. Yeaman S, Aeschbacher S, Bürger R. 2016 The evolution of genomic islands by increased establishment probability of linked alleles. *Mol. Ecol.* **25**, 2542–2558. (doi:10.1111/mec.13611)
33. Coughlan JM, Willis JH. 2019 Dissecting the role of a large chromosomal inversion in life history divergence throughout the *Mimulus guttatus* species complex. *Mol. Ecol.* **28**, 1343–1357. (doi:10.1111/mec.14804)
34. Feder JL, Nosil P. 2009 Chromosomal inversions and species differences: when are genes affecting adaptive divergence and reproductive isolation expected to reside within inversions? *Evolution* **63**, 3061–3075. (doi:10.1111/j.1558-5646.2009.00786.x)
35. Acton AB. 1958 The gene contents of overlapping inversions. *Am. Nat.* **92**, 57–58. (doi:10.1086/282009)
36. Acton AB. 1957 Chromosome inversions in natural populations of *Chirnomus tentans*. *J. Genet.* **55**, 61. (doi:10.1007/BF02981616)
37. Levitan M. 1958 Non-random association of inversions. *Cold Spring Harb. Symp. Quant. Biol.* **23**, 251–268. (doi:10.1101/SQB.1958.023.01.027)
38. Pegueroles C, Aquadro CF, Mestres F, Pascual M. 2013 Gene flow and gene flux shape evolutionary patterns of variation in *Drosophila subobscura*. *Heredity* **110**, 520–529. (doi:10.1038/hdy.2012.118)
39. Kamdem C, Fouet C, White BJ. 2017 Chromosome arm-specific patterns of polymorphism associated with chromosomal inversions in the major African malaria vector, *Anopheles funestus*. *Mol. Ecol.* **26**, 5552–5566. (doi:10.1111/mec.14335)
40. Wallace B. 1953 On coadaptation in *Drosophila*. *Am. Nat.* **87**, 343–358. (doi:10.1086/281795)
41. Haller BC, Messer PW. 2019 SLiM 3: forward genetic simulations beyond the Wright–Fisher model. *Mol. Biol. Evol.* **36**, 632–637. (doi:10.1093/molbev/msy228)
42. Messer PW, Petrov DA. 2013 Population genomics of rapid adaptation by soft selective sweeps. *Trends Ecol. Evol.* **28**, 659–669. (doi:10.1016/j.tree.2013.08.003)
43. Danecek P *et al*. 2011 The variant call format and VCFtools. *Bioinformatics* **27**, 2156–2158. (doi:10.1093/bioinformatics/btr330)
44. Blanquart F, Kaltz O, Nuismer SL, Gandon S. 2013 A practical guide to measuring local adaptation. *Ecol. Lett.* **16**, 1195–1205. (doi:10.1111/ele.12150)
45. Whitlock MC, Lotterhos KE. 2015 Reliable detection of loci responsible for local adaptation: inference of a null model through trimming the distribution of F_{ST}. *Am. Nat.* **186**, S24–S36. (doi:10.1086/682949)
46. Luu K, Bazin E, Blum MGB. 2017 pcadapt: an R package to perform genome scans for selection based on principal component analysis. *Mol. Ecol. Resour.* **17**, 67–77. (doi:10.1111/1755-0998.12592)
47. Roesti M, Hendry AP, Salzburger W, Berner D. 2012 Genome divergence during evolutionary diversification as revealed in replicate lake-stream stickleback population pairs. *Mol. Ecol.* **21**, 2852–2862. (doi:10.1111/j.1365-294X.2012.05509.x)
48. Renaut S, Grassa CJ, Yeaman S, Moyers BT, Lai Z, Kane NC, Bowers JE, Burke JM, Rieseberg LH. 2013 Genomic islands of divergence are not affected by geography of speciation in sunflowers. *Nat. Commun.* **4**, 1827. (doi:10.1038/ncomms2833)
49. Samuk K, Owens GL, Delmore KE, Miller SE, Rennison DJ, Schluter D. 2017 Gene flow and selection interact to promote adaptive divergence in regions of low recombination. *Mol. Ecol.* **26**, 4378–4390. (doi:10.1111/mec.14226)
50. Feder JL, Gejji R, Yeaman S, Nosil P. 2012 Establishment of new mutations under divergence and genome hitchhiking. *Phil. Trans. R. Soc. B* **367**, 461–474. (doi:10.1098/rstb.2011.0256)
51. Koch EL, Ravinet M, Westram AM, Johannesson K, Butlin RK. Submitted. Genetic architecture of repeated phenotypic divergence in *Littorina saxatilis*. *Evolution*.
52. Kim K-W, De-Kayne R, Gordon IJ, Saitoti K, Martins DJ, ffrench-Constant R, Martin S. 2022 Stepwise evolution of a butterfly supergene via duplication and inversion. *Phil. Trans. R. Soc. B* **377**, 20210207. (doi:10.1098/rstb.2021.0207)
53. Kay T, Helleu Q, Keller L. 2022 Iterative evolution of supergene-based social polymorphism in ants. *Phil. Trans. R. Soc. B* **377**, 20210196. (doi:10.1098/rstb.2021.0196)
54. Navarro A, Betrán E, Barbadilla A, Ruiz A. 1997 Recombination and gene flux caused by gene conversion and crossing over in inversion heterokaryotypes. *Genetics* **146**, 695–709. (doi:10.1093/genetics/146.2.695)
55. Miller DE *et al*. 2012 A whole-chromosome analysis of meiotic recombination in *Drosophila melanogaster*. *Genes Genomes Genet.* **2**, 249–260. (doi:10.1534/g3.111.001396)
56. Rieseberg LH. 2001 Chromosomal rearrangements and speciation. *Trends Ecol. Evol.* **16**, 351–358. (doi:10.1016/S0169-5347(01)02187-5)
57. Hoffmann AA, Rieseberg LH. 2008 Revisiting the impact of inversions in evolution: from population genetic markers to drivers of adaptive shifts and speciation? *Annu. Rev. Ecol. Evol. Syst.* **39**, 21–42. (doi:10.1146/annurev.ecolsys.39.110707.173532)
58. Noor MA, Grams KL, Bertucci LA, Reiland J. 2001 Chromosomal inversions and the reproductive isolation of species. *Proc. Natl Acad. Sci. USA* **98**, 12 084–12 088. (doi:10.1073/pnas.221274498)
59. Jay P, Chouteau M, Whibley A, Bastide H, Llaurens V, Parrinello H, Joron M. 2019 Mutation accumulation in chromosomal inversions maintains wing pattern polymorphism in a butterfly. *bioRxiv*, 736504. (doi:10.1101/736504)
60. Mérot C, Llaurens V, Normandeau E, Bernatchez L, Wellenreuther M. 2020 Balancing selection via life-history trade-offs maintains an inversion polymorphism in a seaweed fly. *Nat. Commun.* **11**, 670. (doi:10.1038/s41467-020-14479-7)
61. Stenløkk KSR *et al.* 2022 The emergence of supergenes from inversions in Atlantic salmon. *Phil. Trans. R. Soc. B* **377**, 20210195. (doi:10.1098/rstb.2021.0195)
62. Schaal SM, Haller BC, Lotterhos KE. 2022 Data from: Inversion invasions: when the genetic basis of local adaptation is concentrated within inversions in the face of gene flow. Dryad Digital Repository. (doi:10.5061/dryad.mkkwh712q)